



Finite element formulation of a phase field model based on the concept of generalized stresses

Kais Ammar^{a,*}, Benoît Appolaire^b, Georges Cailletaud^a, Frederic Feyel^{a,c}, Samuel Forest^a

^a Mines ParisTech, Centre des Matériaux/CNRS UMR 7633, 10 rue Desbrueres, BP 87, 91003 Evry Cedex, France

^b LSG2M, École des Mines de Nancy, Parc de Saurupt, 54042 Nancy Cedex, France

^c ONERA, DMSE/CEMN, 29 Ave Div Leclerc, BP 72, 92322 Chatillon, France

ARTICLE INFO

Article history:

Received 8 April 2008

Received in revised form 8 September 2008

Accepted 9 September 2008

Available online 31 October 2008

PACS:

02.70.Dh

05.70.-a

81.65.Mq

46.15.-x

Keywords:

Phase field

Microforce balance

Principle of virtual power

Finite element method

Oxidation

Zirconium

ABSTRACT

A finite element formulation of a phase field model for alloys is proposed within the general framework of continuum thermodynamics in conjunction with the concept of generalized stresses as proposed by Gurtin [1]. Using the principles of the thermodynamics of irreversible processes, balance and constitutive equations are clearly separated in the formulation. Also, boundary conditions for the concentration and order parameter and their dual quantities are clearly stated. The theory is shown to be well-suited for a finite element formulation of the initial boundary value problem. The set of coupled evolution equations, which are the phase field equation and the balance of mass, is solved using an implicit finite element method for space discretization and a finite difference method for time discretization. For an illustrative purpose, the model is used to investigate the growth of an oxide layer at the surface of a pure zirconium slab. Calculations in 1D show a good agreement with an analytical solution for the growth kinetics. Then, 2D calculations of the same process have been undertaken to investigate morphological stability of the oxide layer in order to show the ability of the finite element method to handle arbitrary conditions on complex boundaries.

© 2008 Elsevier B.V. All rights reserved.

1. Introduction

A continuum thermodynamics framework was proposed in [1] to formulate phase field models accounting for the diffusion of chemical species and phase changes. According to this theory, an additional balance equation for generalized stresses, called microforces in the original theory and associated with the order parameter and its first gradient, is postulated. A clear separation is enforced between basic balance laws, which are general and hold for large classes of materials behaviour, and constitutive equations which are material specific. Consequently, the derivation of the appropriate material constitutive relationships can be further generalized in the presence of dissipative processes such as heat transfer and plastic deformation. This formulation can be applied to finite size non-periodic samples and heterogeneous materials

where the initial conditions and the boundary/interface conditions for the concentration and order parameter must be clearly stated.

The finite element method is generally well-suited for handling such initial boundary value problems on finite size specimens, in contrast to the Fourier methods classically used for heterogeneous microstructures with periodicity conditions [2]. Previous attempts to apply the finite element method to phase transformations problems have been presented in [3] for solving Cahn–Hilliard equation, in [4] for the simulation of solidification processes and in [5] for ferroelectric materials.

The objective of the present work is to derive a finite element formulation for the phase field diffusion problem from the thermodynamic formulation based on generalized stresses. It will be shown that this enables the use of large classes of constitutive equations and that it fits into the general computational thermo-mechanical framework used in engineering mechanics as presented in [6].

The present model belongs to the class of diffuse interface models, where the local state of an inhomogeneous microstructure is described by a conservative concentration field c and a non-conservative

* Corresponding author.

E-mail addresses: kais.ammar@ensmp.fr (K. Ammar), benoit.appolaire@mine-np.inpl-nancy.fr (B. Appolaire), georges.cailletaud@ensmp.fr (G. Cailletaud), frederic.feyel@onera.fr (F. Feyel), samuel.forest@ensmp.fr (S. Forest).

vative field ϕ associated with the crystalline nature of the phases, the so-called order parameter. It is based on the time-dependent Ginzburg–Landau equation:

$$\beta \dot{\phi} = \alpha \Delta \phi - \frac{\partial f_0}{\partial \phi} \quad (1)$$

In the phase field approach, the free energy density for an inhomogeneous system can be approximated by the Ginzburg–Landau coarse-grained free energy functional, which contains a local free energy density $f_0(c, \phi)$ and a gradient energy term:

$$f(c, \phi) = f_0(c, \phi) + \frac{\alpha}{2} \nabla \phi \cdot \nabla \phi \quad (2)$$

where the usual specific quadratic contribution with respect to $\nabla \phi$ is adopted here but can be generalized if needed.

The article is organized as follows. First, a generalized principle of virtual power is postulated involving generalized stresses. It is used to derive the balance equations for generalized stresses. The introduced power of internal forces then appears in the energy balance equation. The energy and entropy principles of continuum thermodynamics are explicated in the isothermal case. Second, the clear analogy between the proposed variational formulation and that of conventional computational mechanics leads us to the derivation of an implicit finite element scheme to solve the considered initial boundary value problem, based on time and space discretizations. Finally the method is applied to the prediction of the kinetics of the growth of an oxide layer on zirconium. The finite element method is suitable to study in particular the effect of initial free surface roughness on subsequent oxidation.

2. Balance of generalized stresses and fundamental statements of thermodynamics

2.1. Principle of virtual power

The method of virtual power provides a systematic and straightforward way of deriving balance equations and boundary conditions in various physical situations [7,8]. The application of this principle to an isolated region requires the determination of the virtual powers of the system of generalized forces applied on the body, in which the generalized stresses are not introduced directly but by the value of the virtual power they produce for a given virtual order parameter ϕ^* . Note that macroscopic mechanical effects are not introduced in this work. The wording “generalized forces and stresses” is associated with primarily chemical events contributing to the energy equation and correspond to the notion of microforce in [1].

Guided by Gurtin’s theory [1], we suppose the existence of a system of generalized forces, defined by a scalar internal microstress π and a vector microstress $\underline{\xi}$ that perform work in conjunction with changes in the configurations of atoms, characterized by the order parameter ϕ and its first gradient. The virtual power of internal generalized forces is defined by the integral over the volume V of a power density, which is assumed a priori to be a linear form represented by the generalized stress measures π and $\underline{\xi}$:

$$\mathcal{P}^{(i)}(\phi^*, V) = \int_V (\pi \phi^* - \underline{\xi} \cdot \nabla \phi^*) \, dv \quad (3)$$

$$= \int_V (\pi + \nabla \cdot \underline{\xi}) \phi^* \, dv - \int_{\partial V} (\underline{\xi} \cdot \underline{n}) \phi^* \, ds \quad (4)$$

The next step is to introduce the virtual power of external forces applied to the considered body. It can be split into a virtual power density of long range volume forces, which can include, in general, a volume density of scalar external microforce γ and vector external microforce $\underline{\gamma}$:

$$\mathcal{P}^{(e)}(\phi^*, V) = \int_V (\gamma \phi^* + \underline{\gamma} \cdot \nabla \phi^*) \, dv \quad (5)$$

$$= \int_V (\gamma - \nabla \cdot \underline{\gamma}) \phi^* \, dv + \int_{\partial V} (\underline{\gamma} \cdot \underline{n}) \phi^* \, ds \quad (6)$$

and a virtual power density of generalized contact forces, schematically represented by a surface density ζ of microtraction:

$$\mathcal{P}^{(c)}(\phi^*, V) = \int_{\partial V} \zeta \phi^* \, ds \quad (7)$$

We do not envisage here a possible power of inertial microforces ($\mathcal{P}^{(a)}(\phi^*, V) = 0$). According to the principle of virtual power, the total virtual power of all forces vanishes on any subdomain $\mathcal{D} \subset V$ and for any virtual order parameter field ϕ^* :

$$\forall \phi^*, \quad \forall \mathcal{D} \subset V$$

$$\mathcal{P}^{(i)}(\phi^*, \mathcal{D}) + \mathcal{P}^{(c)}(\phi^*, \mathcal{D}) + \mathcal{P}^{(e)}(\phi^*, \mathcal{D}) + \mathcal{P}^{(a)}(\phi^*, \mathcal{D}) = 0 \quad (8)$$

$$\int_{\mathcal{D}} (\pi + \nabla \cdot \underline{\xi} + \gamma - \nabla \cdot \underline{\gamma}) \phi^* \, dv + \int_{\partial \mathcal{D}} (\zeta - \underline{\xi} \cdot \underline{n} + \underline{\gamma} \cdot \underline{n}) \phi^* \, ds = 0 \quad (9)$$

This identity can be satisfied for any field ϕ^* and $\forall \mathcal{D}$ if and only if:

$$\nabla \cdot (\underline{\xi} - \underline{\gamma}) + \pi + \gamma = 0 \quad \text{in } V \quad (10)$$

$$\zeta = (\underline{\xi} - \underline{\gamma}) \cdot \underline{n} \quad \text{on } \partial V \quad (11)$$

Eq. (10) expresses the general form of balance of generalized stresses. It is identical with Gurtin’s balance of microforces, except the external microforce contribution $\underline{\gamma}$ that may exist in general. In the remainder of this work, however, it is assumed that $\gamma = 0$ and $\underline{\gamma} = 0$ for the sake of brevity. Eq. (11) represents the boundary condition for the generalized traction vector.

2.2. State laws and dissipation potential

According to the first principle of thermodynamics, the time variation of the total energy in a material subdomain is equal to the power of external forces acting on it. In the absence of inertial forces, the total energy is reduced to the internal energy with density e . Then, the energy balance is stated as

$$\int_V \dot{e} \, dv = \mathcal{P}^{\text{ext}} = \int_{\partial V} (\underline{\xi} \cdot \underline{n}) \dot{\phi} \, ds = \int_V \nabla \cdot (\underline{\xi} \dot{\phi}) \, dv \quad (12)$$

This identity is valid for any subdomain $\mathcal{D} \subset V$. The local form of the energy balance is obtained:

$$\dot{e} = \nabla \cdot (\dot{\phi} \underline{\xi}) \quad (13)$$

The second principle, called the entropy principle, is formulated as follows:

$$\int_V \dot{s} \, dv \geq - \int_{\partial V} \underline{\Phi} \cdot \underline{n} \, ds \quad \text{and} \quad \underline{\Phi} = -\mu \frac{\underline{J}}{T} \quad (14)$$

where s is the entropy density, $\underline{\Phi}$ the entropy flux, \underline{J} the diffusion flux and μ the diffusion potential.

Using the equation of local conservation of mass:

$$\dot{c} = -\nabla \cdot \underline{J} \quad (15)$$

we obtain the following local form of the entropy inequality:

$$T\dot{s} - \nabla \cdot (\mu \underline{J}) \geq 0 \quad (16)$$

Combining the equation of the free energy density $\dot{f} = \dot{e} - T\dot{s}$ in the isothermal case with Eqs. (13)–(16), leads to the Clausius–Duhem inequality:

$$-\dot{f} - \pi \dot{\phi} + \underline{\xi} \cdot \nabla \dot{\phi} - \underline{J} \cdot \nabla \mu - \mu \nabla \cdot \underline{J} \geq 0 \quad (17)$$

The free energy density is assumed to be a function of concentration c , order parameter ϕ , as well as its gradient $\nabla\phi$. The Clausius–Duhem inequality can then be written as follows:

$$\left(\mu - \frac{\partial f}{\partial c}\right)\dot{c} - \left(\pi + \frac{\partial f}{\partial \phi}\right)\dot{\phi} + \left(\underline{\xi} - \frac{\partial f}{\partial \nabla\phi}\right) \cdot \nabla\dot{\phi} - \underline{J} \cdot \nabla\mu \geq 0 \quad (18)$$

For every admissible process and for any given $(c, \phi, \nabla\phi)$, the inequality (18) must hold for arbitrary values of \dot{c} , $\dot{\phi}$ and $\nabla\dot{\phi}$. The microstress $\underline{\xi}(c, \phi, \nabla\phi)$ and the diffusion potential $\mu(c, \phi, \nabla\phi)$ are assumed independent of $\nabla\dot{\phi}$ and \dot{c} , in which these latter appear linearly in the inequality above (see e.g. [9,10]). The following state laws are deduced:

$$\mu = \frac{\partial f}{\partial c} = \frac{\partial f_0}{\partial c} \quad (19)$$

$$\underline{\xi} = \frac{\partial f}{\partial \nabla\phi} = \alpha \nabla\phi \quad (20)$$

when the specific form (2) is adopted. The Clausius–Duhem inequality then reduces to the residual dissipation:

$$D = -\underline{J} \cdot \nabla\mu - \pi_{\text{dis}}\dot{\phi} \geq 0 \quad \text{with} \quad \pi_{\text{dis}} = \pi + \frac{\partial f}{\partial \phi} \quad (21)$$

where π_{dis} is the chemical force associated with the dissipative processes, as introduced in [1].

In order to define the complementary laws related to the dissipative processes, we postulate the existence of a dissipation potential function $\Omega(\nabla\mu, \pi_{\text{dis}})$. The retained specific form is the following:

$$\Omega(\nabla\mu, \pi_{\text{dis}}) = \frac{1}{2}L(\phi)\nabla\mu \cdot \nabla\mu + \frac{1}{2}(1/\beta)\pi_{\text{dis}}^2 \quad (22)$$

where $L(\phi)$ and β are material parameters or functions.

The complementary evolution laws derive from the dissipation potential:

$$\dot{\phi} = -\frac{\partial \Omega}{\partial \pi_{\text{dis}}} = -(1/\beta)\pi_{\text{dis}} \quad (23)$$

$$\underline{J} = -\frac{\partial \Omega}{\partial \nabla\mu} = -L(\phi)\nabla\mu \quad (24)$$

The convexity of the dissipation potential ensures the positivity of dissipation.

Combining Eqs. (21) and (23), we get

$$\pi = -\beta\dot{\phi} - \frac{\partial f}{\partial \phi} \quad (25)$$

The substitution of the two state laws and the complementary laws, into the balance equations for mass concentration and generalized stresses respectively leads to the evolution equations for concentration and order parameter:

$$\dot{c} = -\nabla \cdot (-L(\phi)\nabla\mu) = -\nabla \cdot \left(-L(\phi)\nabla \frac{\partial f}{\partial c}\right) \quad (26)$$

$$\nabla \cdot \underline{\xi} + \pi = -\beta\dot{\phi} + \alpha\Delta\phi - \frac{\partial f}{\partial \phi} = 0 \quad (27)$$

The usual diffusion and Ginzburg–Landau equations are thus retrieved.

3. Finite element implementation

3.1. Variational formulation

The variational formulation of the phase field partial differential equation directly follows from the formulated principle of virtual power (8):

$$\mathfrak{Z}(\phi^{\star}) = \int_V (\pi\phi^{\star} - \underline{\xi} \cdot \nabla\phi^{\star}) dv + \int_{\partial V} \zeta\phi^{\star} ds = 0 \quad (28)$$

On the other hand, the usual weak form of the diffusion equation is recalled:

$$\mathfrak{Z}(c^{\star}) = \int_V (\dot{c}c^{\star} - \underline{J} \cdot \nabla c^{\star}) dv + \int_{\partial V} jc^{\star} ds = 0 \quad (29)$$

where c^{\star} is an arbitrary field of virtual concentration.

Accordingly, the phase field problem can be formulated as follows:

$$\begin{aligned} &\text{find } \{c(\mathbf{x}, t), \phi(\mathbf{x}, t)\} \text{ satisfying} \\ &\text{at } t = 0 \\ &\quad c(\mathbf{x}, 0) = c_0(\mathbf{x}) \\ &\quad \phi(\mathbf{x}, 0) = \phi_0(\mathbf{x}) \\ &\text{at each instant } t > 0 \\ &\quad \mathfrak{Z}(c^{\star}) = \int_V (\dot{c}c^{\star} - \underline{J} \cdot \nabla c^{\star}) dv + \int_{\partial V} jc^{\star} ds = 0 \\ &\quad \mathfrak{Z}(\phi^{\star}) = \int_V (\pi\phi^{\star} - \underline{\xi} \cdot \nabla\phi^{\star}) dv + \int_{\partial V} \zeta\phi^{\star} ds = 0 \end{aligned} \quad (30)$$

3.2. Discretization

In order to obtain a finite element solution, the spatial domain is subdivided into N elements. The nodal degrees of freedom are the values at nodes of phase and concentration. The fields c and ϕ are approximated within each element and at every time t , in terms of nodal values by means of interpolation functions, within each element:

$$\begin{aligned} c(\mathbf{x}, t) &= \sum_{i=1}^n N_i^e(\mathbf{x})c_i(t), & \phi(\mathbf{x}, t) &= \sum_{i=1}^n N_i^e(\mathbf{x})\phi_i(t) \\ c^{\star}(\mathbf{x}, t) &= \sum_{i=1}^n N_i^e(\mathbf{x})c_i^{\star}(t), & \phi^{\star}(\mathbf{x}, t) &= \sum_{i=1}^n N_i^e(\mathbf{x})\phi_i^{\star}(t) \\ \nabla c(\mathbf{x}, t) &= \sum_{i=1}^n B_i^e(\mathbf{x})c_i(t), & \nabla\phi(\mathbf{x}, t) &= \sum_{i=1}^n B_i^e(\mathbf{x})\phi_i(t) \end{aligned}$$

where n is the number of nodes in the element e containing \mathbf{x} and the shape functions are denoted by N_i . The matrix $[B^e(\mathbf{x})]$ is defined by the first derivatives of the shape functions, which read in the 2D case:

$$[B^e(\mathbf{x})] = \begin{bmatrix} \frac{\partial N_1^e}{\partial x} & \frac{\partial N_2^e}{\partial x} & \dots & \frac{\partial N_n^e}{\partial x} \\ \frac{\partial N_1^e}{\partial y} & \frac{\partial N_2^e}{\partial y} & \dots & \frac{\partial N_n^e}{\partial y} \end{bmatrix} \quad (31)$$

Regarding time discretization, the Euler implicit method is applied. Using the notation $c(t)$ and $\phi(t)$ for the known values of the current time step t , $\phi(t + \Delta t)$ and $c(t + \Delta t)$ at time $t + \Delta t$ are estimated by solving the following equations:

$$\dot{c}(t + \Delta t) = \frac{c(t + \Delta t) - c(t)}{\Delta t} \quad (32)$$

$$\dot{\phi}(t + \Delta t) = \frac{\phi(t + \Delta t) - \phi(t)}{\Delta t} \quad (33)$$

$$c(0) = c_0, \quad \phi(0) = \phi_0 \quad (34)$$

Δt indicates the time increment, and c_0, ϕ_0 are the initial conditions for the concentration and order parameter.

After substituting the nodal approximation and the time discretization into Eq. (30), we deduce the element residual, which can be written in the following form:

$$\{R^e(c, \phi)\} = \begin{Bmatrix} R_c^e(c, \phi) \\ R_\phi^e(c, \phi) \end{Bmatrix} \quad (35)$$

where $R_c^e(c, \phi)$ and $R_\phi^e(c, \phi)$ are respectively the element residuals for the variational formulation of classical diffusion (29) and phase field (28), defined as follow:

$$(R_c^e)_i = \int_{V^e} N_i^e N_j^e \dot{c}_j^e - [B^e]_{ij} J_j \, dv + \int_{\partial V^e} N_i^e j_j \, ds \quad (36)$$

$$(R_\phi^e)_i = \int_{V^e} N_i^e \pi(\phi) - [B^e]_{ij} \zeta_j \, dv + \int_{\partial V^e} N_i^e \zeta_j \, ds \quad (37)$$

The global residual vector can be obtained by assembling the element residuals for all finite elements using the matrix assembly $[A^e]$:

$$\{R(\phi)\} = \sum_{e=1}^N [A^e] \cdot \{R^e(\phi)\} = \{0\} \quad (38)$$

following the usual definition in computational mechanics [6].

Given a known set of nodal degrees of freedom at time t , and assuming that the residual vanishes at the next time step $t + \Delta t$, a set of non-linear equations results for the nodal degrees of freedom at $t + \Delta t$. It is solved with the Newton–Raphson method in an iterative manner. This requires the computation of the element generalized stiffness matrix which is obtained by derivation of the residual vector with respect to the degrees of freedom (c, ϕ) :

$$[K_t^e] = \begin{bmatrix} \partial R^e / \partial \delta^e \\ \partial R^e / \partial c^e \end{bmatrix} = \begin{bmatrix} [K_{cc}^e] & [K_{c\phi}^e] \\ [K_{\phi c}^e] & [K_{\phi\phi}^e] \end{bmatrix} \quad (39)$$

$$\text{with } \{\delta^e\} = \begin{Bmatrix} \{c^e\} \\ \{\phi^e\} \end{Bmatrix}$$

The element generalized stiffness matrix is divided into four sub-matrices. Referring to Eqs. (36) and (37), the individual components $(K_{cc}^e)_{ij}$, $(K_{c\phi}^e)_{ij}$, $(K_{\phi c}^e)_{ij}$ and $(K_{\phi\phi}^e)_{ij}$ are

$$(K_{cc}^e)_{ij} = \frac{\partial (R_c^e)_i}{\partial c_j^e} = \int_{V^e} \frac{1}{\Delta t} N_i^e N_j^e - [B^e]_{ik} \left[\frac{\partial J}{\partial c^e} \right]_{kj} \, dv \quad (40)$$

$$(K_{c\phi}^e)_{ij} = \frac{\partial (R_c^e)_i}{\partial \phi_j^e} = \int_{V^e} -[B^e]_{ik} \left[\frac{\partial J}{\partial \phi^e} \right]_{kj} \, dv \quad (41)$$

$$(K_{\phi c}^e)_{ij} = \frac{\partial (R_\phi^e)_i}{\partial c_j^e} = \int_{V^e} N_i^e \left(\frac{\partial \pi}{\partial c^e} \right)_j \, dv \quad (42)$$

$$(K_{\phi\phi}^e)_{ij} = \frac{\partial (R_\phi^e)_i}{\partial \phi_j^e} = \int_{V^e} N_i^e \left(\frac{\partial \pi}{\partial \phi^e} \right)_j - [B^e]_{ik} \left[\frac{\partial \zeta}{\partial \phi^e} \right]_{kj} \, dv \quad (43)$$

The elements used in this work are linear elements and quadratic elements with reduced integration (4 Gauss points in square elements for instance).

4. Results

4.1. Parameters

Following Kim et al. [11], the free energies of the two-phases are interpolated for intermediate values of ϕ with a polynomial $h(\phi)$ varying in a monotonic way between both phases. To this free energy landscape, a double well potential $g(\phi)$ is added, accounting for the free energy penalty of the interface.

$$f_0(c, \phi) = \psi(c, \phi) + Wg(\phi) \quad (44)$$

where $\psi(c, \phi) = h(\phi)f_1(c) + [1 - h(\phi)]f_2(c)$. The specific polynomials $g(\phi) = \phi^2(1 - \phi)^2$ and $h(\phi) = \phi^2(3 - 2\phi)$ have been chosen as commonly done in previous works [12].

For simplicity, the free energy densities of both phases f_1 and f_2 have been described by simple quadratic functions of the concentration c [13]:

$$f_i(c) = \frac{1}{2} k_i (c - A_i)^2 \quad (45)$$

where $i = \{1, 2\}$ denotes phase 1 or 2.

The constants k_1, k_2 are the curvatures of the free energies with respect to concentration (positive to avoid any spinodal decompo-

sition); A_1, A_2 are the equilibrium concentrations of both phases delimiting the two-phases region in the phase diagram, and corresponding to the minima of f_1 and f_2 for the particular quadratic functions chosen.

The phase field parameters α and W have been related to the interface energy and thickness, respectively σ and δ . As noted by Kim et al. [11], there are in general two contributions to the interfacial energy: the first one coming from the double well function $g(\phi)$, the second one coming from the variation in concentration within the interface. Indeed, at a plane interface at equilibrium, Eq. (1) becomes:

$$\alpha \frac{d^2 \phi_{eq}}{dx^2} = \frac{\partial f_0}{\partial \phi_{eq}} \quad (46)$$

where x is the distance normal to the interface. This equation can be integrated to get the phase field at equilibrium $\phi_{eq}(x)$, by noting that the right hand side of Eq. (46) can be transformed into the differential of the grand potential $\omega = f - \mu_{eq}c$ where μ_{eq} is the diffusion potential at equilibrium [11]. Indeed:

$$d\omega = \frac{\partial \omega}{\partial \phi} d\phi \quad (47)$$

because $\partial f / \partial c = \mu_{eq}$. This leads to the following relationship:

$$\sigma = \sqrt{2\alpha} \int_0^1 \sqrt{\omega(\phi_{eq}) - \omega(0)} \, d\phi_{eq} \quad (48)$$

where $\omega(\phi_{eq}) - \omega(0) = \psi(c(\phi_{eq}), \phi_{eq}) + Wg(\phi_{eq})$. Because the magnitude of $\psi(c(\phi_{eq}), \phi_{eq})$ scales with the curvatures k_i , we have chosen $k_1 V_m = k_2 V_m = 1$ J/mole, where V_m is the molar volume. This leads to a very small contribution of the concentration profile compared to that of the double well term $Wg(\phi)$. Neglecting $\psi(c(\phi_{eq}), \phi_{eq})$ in $\omega(\phi_{eq})$ gives the standard result:

$$\sigma = \sqrt{\alpha W} / (3\sqrt{2}) \quad (49)$$

$$\delta = 2.94 \sqrt{2\alpha/W} \quad (50)$$

where 2.94 in the last relation comes from the way the interface width δ has been defined, i.e. for values of ϕ in the range [0.05;0.95]. It must be noted that taking values for k_1 and k_2 of the same order of magnitude as W would disqualify Eq. (50) for relating the interfacial energy and the double well height W . Of course, this could have some large effects on the results, especially on the phenomena involving interface curvatures, such as morphological stabilization/destabilization as studied in the following subsection.

The Onsager coefficient $L(\phi)$ is defined with respect to the chemical diffusivities D_1 and D_2 in both phases by means of the interpolation function $h(\phi)$:

$$L(\phi) = h(\phi)D_1/k_1 + (1 - h(\phi))D_2/k_2 \quad (51)$$

where the k_i ensure that Fick's law is recovered in the bulk phases. Finally, the phase field mobility $1/\beta$ has been set by successive trials with decreasing β such as to obtain a diffusion controlled mode of growth.

Table 1
Parameters and data used for the zirconium–oxygen system at 350 °C

β (Js/m ³)	1.78×10^5	
σ (J/m ²)	0.1	
δ (m)	7×10^{-8}	
α (J/m)	7.14×10^{-9}	
W (J/m ³)	2.5×10^7	
V_m (m ³ /mole)	10^{-5}	
Phase	Zr ($i = 1$)	ZrO ₂ ($i = 2$)
A_i (mole fraction)	0.24	0.66
$k_i V_m$ (J/mole)	1	1
D_i (m ² /s) from [15]	1.722×10^{-20}	6.368×10^{-18}

4.2. Oxidation of zirconium

The model has been implemented in the finite element code ZeBuLoN and used to study the growth of oxide layers in α phase at 350 °C in the simple Zr–O binary system. The parameters are reported in Table 1. An interfacial energy of 100 mJ/m² corresponds to a coherent/semi-coherent interface between the oxide and zirconium [14]. An interface thickness δ about two orders of magnitude larger than a realistic value has been chosen to render the computations tractable.

A regular mesh with 1000 linear elements has been used to discretize a 1 μm long 1D slab. An adaptive time step implemented in ZeBuLoN as a standard option has been used for the calculations: small time steps of the order of 10^{-6} s were necessary to achieve a good convergence at the beginning of the process, whereas large time steps of the order of 10^3 s were reached at the end of the calculations. The following boundary conditions to the system have been applied on the right side: $\xi \cdot \underline{n} = 0$ and $\underline{J} \cdot \underline{n} = 0$; and on the left side corresponding to the surface: $\xi \cdot \underline{n} = 0$ and $c = 0.68$. The Dirichlet condition imposed at the left side is assumed to mimic the reaction between the oxide surface and the oxidizing atmosphere. A value slightly above the stoichiometric concentration has been chosen to rapidly initiate the growth of the layer and shorten an initial transient regime.

A profile of ϕ in tanh has been set corresponding to an initial 84 nm thick ZrO₂ layer at the surface of the zirconium slab. A decreasing concentration profile has been prescribed in ZrO₂ between the surface and the interface at equilibrium. A flat profile is imposed at 0.22 a value below equilibrium in α corresponding to α phase undersaturated in oxygen (Fig. 1).

The concentration profiles are shown at different times in Fig. 1. The steep gradients locate the interface between the oxide and the metal. At the beginning of the process (e.g. the curve after 2 h of isothermal holding), the concentrations at interface are slightly higher than the equilibrium ones (dashed lines), due to the dissipation of free energy associated with interfacial kinetics and with diffusion of oxygen across interface. These dissipation processes are magnified because of the unrealistically large interface width (Table 1), chosen for computational purpose as commonly done in phase field simulations. These spurious effects can be eliminated by performing a careful asymptotics analysis (e.g. [13]) together with using an adaptive mesh refinement technique as discussed thoroughly in [16]. These improvements will be undertaken in a

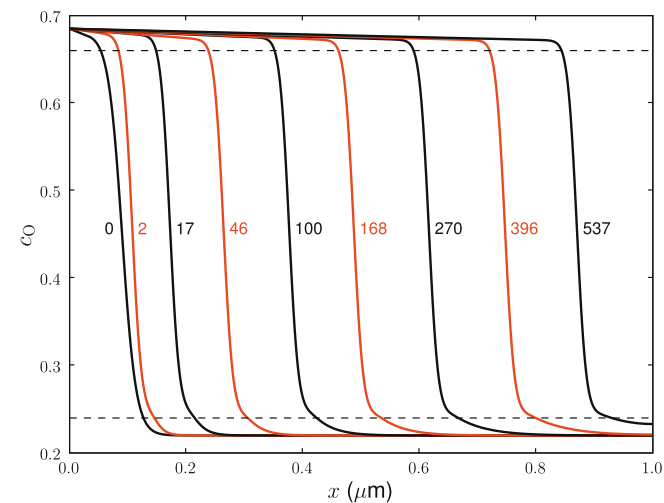


Fig. 1. Evolution of the concentration profile in oxygen (in mole fraction) near the surface of the slab; numbers labelling the curves are the related holding times in hours. Horizontal dashed lines are the equilibrium concentrations.

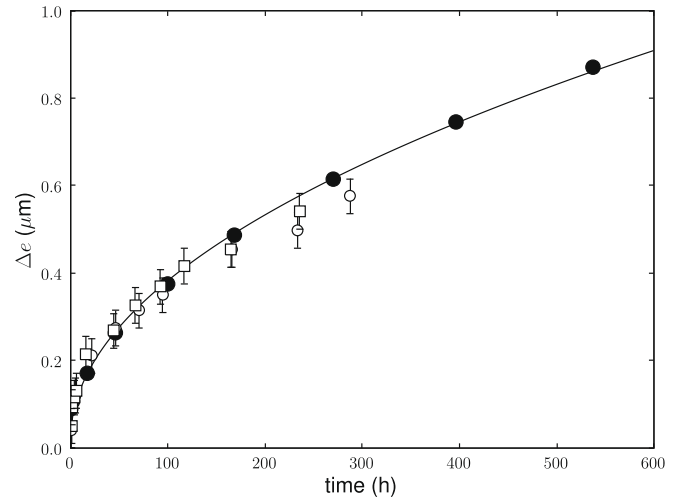


Fig. 2. The growth kinetics of the oxide layer: black dots are related to the profiles in Fig. 1; the continuous line corresponds to the best fit with a parabolic law. Experimental data from [15] obtained in Zircaloy-4 have been superimposed with white symbols.

forthcoming study. Very quickly, a gradient in oxygen content develops in α in front of the growing oxide. The inward growth process is thus driven by diffusion of oxygen in both phases.

The time evolution of the oxide thickness Δe shown in Fig. 2 has been deduced from the profiles by tracking the position of $\phi = 0.5$. Apart from the beginning of the process which is strongly influenced by the initial conditions, the growth law is parabolic, i.e. $\Delta e = K\sqrt{t}$. The growth constant $K = 7.5 \cdot 10^{-10}$ m/s has been determined by linear regression of $(\ln(\Delta e), \ln(t))$, discarding the first points. This value is in good agreement with the value of $7.75 \cdot 10^{-10}$ m/s given by the analytical solution of [17]. The difference can be attributed to the dissipation of the driving force by the interfacial phenomena. Moreover, it must be noticed that a good agreement with the experimental measurements of [15] is achieved, as shown in Fig. 2.

In order to illustrate the advantage of the finite element formulations over the other methods used in phase field modeling, 2D calculations have been performed to investigate a problem where the surface geometry may play a role: the morphological stability

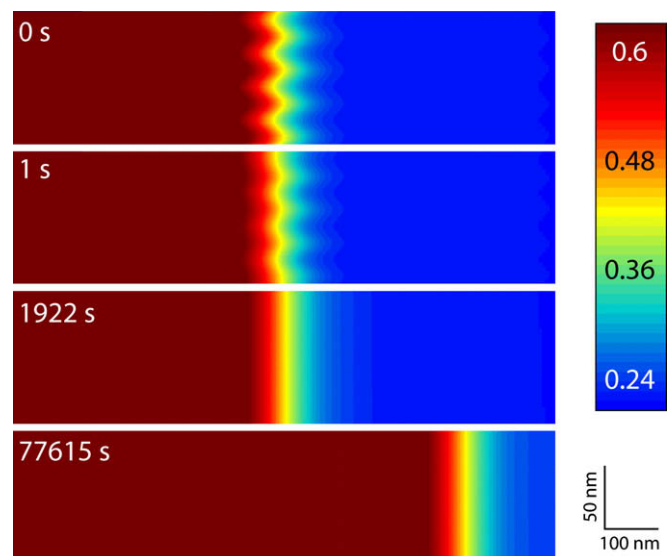


Fig. 3. Evolution vs. time of the concentration field in oxygen during the growth of an oxide with an interface initially destabilized by a sine.

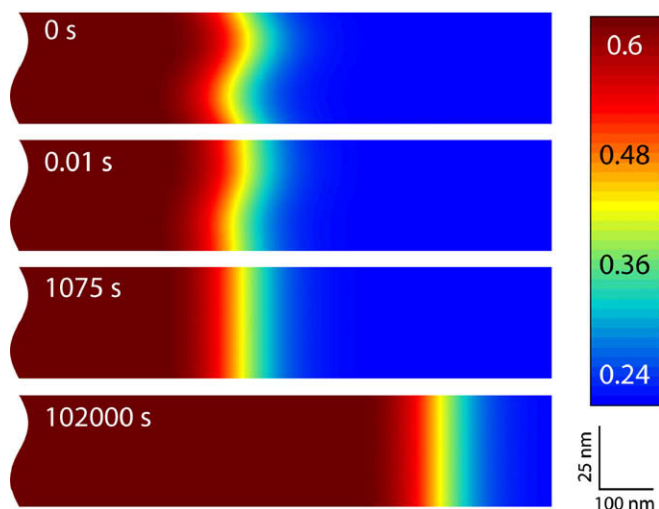


Fig. 4. Evolution vs. time of the concentration field in oxygen during the growth of a sinusoidal oxide layer.

of the oxide layer. The finite element mesh is composed of 15,000 quadrangular linear elements, and time steps similar to the 1D case have been used for the calculations. As shown in [17] for the nitriding of pure iron, the configuration of the diffusion fields has a stabilizing effect with respect to fluctuations, at both the layer/matrix interface and the layer surface. Hence, small sine fluctuations have been imposed initially either at the interface (Fig. 3), or at both surface and interface (Fig. 4), with different wavelengths. In both cases, it is observed that the corrugations have completely disappeared after thousand seconds, i.e. on a short time scale when compared to the growth process. This result is again in accordance with the analytical analysis of a similar problem [17], and shows the potentiality of the present formulation and implementation for the phase field modeling.

5. Conclusion

A finite element formulation for a phase field model for alloys has been presented, based on the introduction of generalized stres-

ses and their balance, and the framework of the thermodynamics of irreversible processes. Using the finite element method to discretize space and the finite difference method to discretize time, numerical simulations were performed to investigate the oxidation kinetics of pure zirconium. Other required validations were performed concerning mesh size and types of elements, which were not reported here.

The formulation, presented here, allows, on the one hand, the application of any arbitrary form for the free energy, such as Folch–Plapp [18] and Khachaturyan models [19] and, on the other hand, the use of finite size samples with arbitrary geometries and for very general non-periodic or periodic boundary conditions. Furthermore, an extension of the present model will be obtained by introducing other general processes that include dissipation, like in the coupling with mechanics, especially plasticity.

References

- [1] M.E. Gurtin, *Physica D* 92 (1996) 178–192.
- [2] L.Q. Chen, S.Y. Hu, in: D. Raabe, F. Roters, F. Barlat, L.Q. Chen (Eds.), *Continuum Scale Simulation of Engineering Materials*, Wiley-VCH, 2004, pp. 271–296.
- [3] P.K. Chan, A.D. Rey, *Computational Materials Sciences* 3 (1995) 377–392.
- [4] D. Danilov, B. Nestler, *Journal of Crystal Growth* 275 (2005) 177–182.
- [5] D. Schrader, R. Mueller, B.X. Xu, D. Gross, *Computer Methods in Applied Mechanics and Engineering* 196 (2007) 4365–4374.
- [6] J. Besson, G. Cailletaud, J.-L. Chaboche, S. Forest, *Mécanique non linéaire des matériaux*, Hermès Sciences, France, 2001.
- [7] P. Germain, *Journal de Mécanique* 12 (1973) 235–274.
- [8] P. Germain, *SIAM Journal on Applied Mathematics* 25 (1973) 556–575.
- [9] B.D. Coleman, W. Noll, *Archive for Rational Mechanics and Analysis* 13 (1963) 167–178.
- [10] B.D. Coleman, M.E. Gurtin, *The Journal of Chemical Physics* 47 (1967) 597–613.
- [11] S.G. Kim, W.T. Kim, T. Suzuki, *Physical Review E* 58 (3) (1998) 3316–3323.
- [12] S.-L. Wang, R.F. Sekerka, A.A. Wheeler, B.T. Murray, S.R. Coriell, R.J. Braun, G.B. McFadden, *Physica D* 69 (1993) 189–200.
- [13] B. Echebarria, R. Folch, A. Karma, M. Plapp, *Physical Review E* 70 (2004) 061604–061626.
- [14] R. Penelle, P. Boisot, G. Béranger, P. Lacombe, *Journal of Nuclear Materials* 30 (1971) 340–342.
- [15] M. Parise, *Mécanismes de corrosion des alliages de zirconium: étude des cinétiques initiales d'oxydation et du comportement mécanique du système métal-oxyde*. Thèse de doctorat, Ecole des Mines de Paris, 1996.
- [16] N. Provatas, M. Greenwood, B. Athreya, N. Goldenfeld, J. Dantzig, *International Journal of Modern Physics B* 19 (2005) 4525–4565.
- [17] B. Appolaire, M. Gouné, *Computational Materials Science* 38 (2006) 126–135.
- [18] R. Folch, M. Plapp, *Physical Review E* 72 (1) (2005) 011602.
- [19] Y. Wang, A.G. Khachaturyan, *Acta Metallurgica et Materialia* 43 (5) (1995) 1837–1857.